Talanta 154 (2016) 208–218

Contents lists available at ScienceDirect

Talanta

journal homepage: www.elsevier.com/locate/talanta

Highly sensitive quantitation of pesticides in fruit juice samples by modeling four-way data gathered with high-performance liquid chromatography with fluorescence excitation-emission detection

Milagros Montemurro [a], Licarion Pinto [b], Germano Véras [c], Adriano de Araújo Gomes [b], María J. Culzoni [a], Mário C. Ugulino de Araújo [b,*], Héctor C. Goicoechea [a,*]

[a] Laboratorio de Desarrollo Analítico y Quimiometría (LADAQ), Cátedra de Química Analítica I, Facultad de Bioquímica y Ciencias Biológicas, Universidad Nacional del Litoral, Ciudad Universitaria, 3000 Santa Fe, Argentina

[b] Laboratório de Automação e Instrumentação em Química Analítica e Quimiometria (LAQA) Universidade Federal da Paraíba, CCEN, Departamento de Química, Caixa Postal 5093, CEP 58051-900 João Pessoa, PB, Brazil

[c] Departamento de Química, Centro de Ciências e Tecnologia, Universidade Estadual da Paraíba, 58.429-500 Campina Grande, PB, Brazil

ARTICLE INFO

Article history:
Received 31 December 2015
Received in revised form
22 March 2016
Accepted 23 March 2016
Available online 25 March 2016

Keywords:
Liquid chromatography
Four-way data array
Pesticides
Fruit juice
Multi-way calibration

ABSTRACT

A study regarding the acquisition and analytical utilization of four-way data acquired by monitoring excitation–emission fluorescence matrices at different elution time points in a fast HPLC procedure is presented. The data were modeled with three well-known algorithms: PARAFAC, U-PLS/RTL and MCR-ALS, the latter conveniently adapted to model third-order data. The second-order advantage was exploited when analyzing samples containing uncalibrated components. The best results were furnished with the algorithm U-PLS/RTL. This fact is indicative of both no peak time shifts occurrence among samples and high colinearity among spectra. Besides, this latent-variable structured algorithm is capable of better handle the need of achieving high sensitivity for the analysis of one of the analytes. In addition, a significant enhancement in both predictions and analytical figures of merit was observed for carbendazim, thiabendazole, fuberidazole, carbofuran, carbaryl and 1-naphtol, when going from second- to third-order data. LODs obtained were ranged between 0.02 and 2.4 μg L^{-1}.

1. Introduction

High performance liquid chromatography (HPLC) combined with fast-scanning fluorescence detection (FSFD) can generate spectral-elution time second-order data [1,2]. The proper modeling of these data can be done not only when full selectivity in the chromatographic separation is not achieved but even in the presence of unexpected constituents in new samples. This modeling gives place to three-way calibration, which has additional benefits such as decreasing cost and time of analysis. Recent pertinent examples can be found in the literature [3–10].

On the other hand, four-way arrays generated with chromatographic systems equipped with proper detection devices can also be exploited for analytical purposes [1]. One common example of four-way/third-order data involving chromatography is comprehensive two-dimensional gas chromatography followed by mass spectrometric detection (GC × GC-TOFMS) [11]. Another approach consists in recording excitation-emission matrices (EEMs) as a function of the elution time. Very recently, this was done for the first time with quantitative purposes by following two different approaches: (a) performing several chromatographic runs, and recording the emission spectra of every one at a different excitation wavelength, across the excitation spectra of the compounds of interest [12], and (b) collecting chromatographic fractions every two seconds and then, obtaining excitation-emission matrices for each collected fraction [13]. On the other hand, liquid chromatography-diode array detection (LC-DAD)-kinetic third order data were modeled by Bezemer and Rutan [14]. In addition, very recently, Qing et al. reported the generation and modeling of fourth-order LC-DAD-pH-kinetic data to study the hydrolysis of naptalam [15].

Since multi-way data of chromatographic origin usually present multi-linearity loss due to time mode variations of constituent profiles from sample to sample, multivariate curve resolution coupled to alternating least squares (MCR-ALS) [16] has been the selected algorithm for modeling such complex data. The original third-order data should be first unfolded into matrices, i.e. arranged into bilinear augmented matrices [11,17], to be modeled with the MCR-ALS algorithm. In addition, a latent structured

* Corresponding authors.
E-mail addresses: laqa@quimica.ufpb.br (M.C. Ugulino de Araújo), hgoico@fbcb.unl.edu.ar (H.C. Goicoechea).

http://dx.doi.org/10.1016/j.talanta.2016.03.078
0039-9140/

model such as partial least squares in its unfolded alternative (U-PLS), and coupled to residual trilinearization (RTL) has been applied to third-order data to exploit the second-order advantage [18,19]. Furthermore, when multi-linearity is fulfilled, parallel factor analysis (PARAFAC) can also be applied [20]. Finally, it should be commented that a new augmented parallel factor analysis (APARAFAC) was successfully proposed by Olivieri and coworkers to circumvent the problem of multi-linearity loss in the time mode [21].

Regarding the target analytes of the present work, it should be noticed that the use of pesticides in agriculture has increased dramatically during the last few decades. Although they offer unquestionable benefits in providing a plentiful, low-cost supply of high-quality fruit and vegetables, their incorrect application may leave harmful residues, which involve possible health risks [22]. For this reason, government and international organizations, such as the European Commission (EC) [23] and the Food and Drug Administration (FDA) [24] have established maximum residue limits (MRLs) to control the use of these potentially harmful compounds.

A literature search reveals that a large number of methods for the determination of pesticides have been published. Specifically, the determination of benzimidazolic pesticides (carbendazim, thiabendazole and fuberidazole) and carbamates (carbaryl, carbofuran and 1-naphthol) have been carried out by fluorescence spectroscopy [25–27], liquid chromatography coupled with diode array detection [28], fluorescence detection [29,30], mass spectrometry [31] and tandem mass spectrometry [32], gas chromatography-mass spectrometry [33], micellar electrokinetic chromatography coupled with mass spectrometry [34] and electrochemical methods [35].

In the present work, we report a method for the quantitation of carbendazim (CBZ), fuberidazole (FBZ), thiabendazole (TBZ), carbofuran (CBF), carbaryl (CBR) and naphthol (NPH) in fruit juice samples based on the generation of third-order chromatographic data and their modeling with three different algorithms. The data were obtained using HPLC coupled with fast-scanning fluorescence detection, recording for each sample several emission-elution time two-way matrices at different excitation wavelengths.

Interestingly, this procedure can be adapted to a high number of complex analytical applications, allowing to extract more information compared to that obtained by recording the emission spectrum at one excitation wavelength selected as a compromise between the optimal wavelength for each analyte. In this way, the optimal signal for every target analyte can be collected, giving the possibility of extracting qualitative information which could be extremely useful for identification of co-eluting compounds in highly complex samples.

2. Theory

2.1. U-PLS-RTL

The original cube-structured data are transformed into unidimensional arrays (vectors) by concatenating (unfolding) the original three-dimensional information. Then, concentration information, included in the vector $\mathbf{y}$ ($I \times 1$), is employed in the calibration step without including data for the unknown sample [36]. As it is well-known for PLS, a set of loadings $\mathbf{P}$ and weight loadings $\mathbf{W}$ ($JKL \times A$, where A is the number of latent variables) as well as regression coefficients $\mathbf{v}$ (size $A \times 1$) are obtained after the calibration step. Usually, the leave-one-out cross-validation procedure is implemented for selecting the parameter A [37]. Subsequently, $\mathbf{v}$ is employed to estimate the analyte concentration through the following equation:

$$y_u = t_u^T v \quad (1)$$

where $\mathbf{t}_u$ (size $A \times 1$) is the test sample score, obtained by projection of the (unfolded) data for the test sample $\boldsymbol{X}_u$ [vec($\boldsymbol{X}_u$)] of size ($JKL \times 1$) onto the space of the A latent factors:

$$t_u = (W^T P)^{-1} W^T \mathrm{vec}(X_u) \quad (2)$$

If the sample contains unexpected components, the scores given by Eq. (2) are not suitable for analyte prediction using Eq. (1), generating abnormally large residuals in comparison with the typical instrumental noise assessed by replicate measurements.

In the latter cases, RTL models the interferent effects with a Tucker3 decomposition [18], i.e. RTL aims at minimizing the norm of the residual vector $\mathbf{e}_u$, computed while fitting the sample data to the sum of the relevant contributions to the sample signal. The Tucker3 model is seen as a way to generalize Principal Component Analysis (PCA) to higher orders. The expression for a single interferent is the following.

$$\mathrm{vec}(\boldsymbol{X}_u) = \mathbf{P}\mathbf{t}_u + g_{int}(d_{int} \otimes \mathbf{c}_{int} \otimes \mathbf{b}_{int}) + \mathbf{e}_u \quad (3)$$

where $\mathbf{b}_{int}$, $\mathbf{c}_{int}$ and $\mathbf{d}_{int}$ are normalized profiles in the three modes for the interference and g_{int} is the first core element, analogous to the first component in PCA, obtained for Tucker3 decomposition of the residual array $\boldsymbol{E}$p in the following way:

$$(g_{int}, \mathbf{b}_{int}, \mathbf{c}_{int}, \mathbf{d}_{int}) = \mathrm{Tucker3}(E_p) \quad (4)$$

During this stage, $\mathbf{P}$ is kept constant at the calibration values and $\mathbf{t}_u$ is varied until $\| \mathbf{e}_u \|$ is minimized by a Gauss-Newton (GN) procedure. Finally, the analyte concentrations are provided by Eq. (1), although the final $\mathbf{t}_u$ ($\mathbf{t}_{uRTL}$) vector found by the RTL procedure is used.

A relevant issue is to know the number of interferents N_i, which can be assessed by comparing the final residuals s_u with the instrumental noise level. Usually, this value is computed for a trial number of components. Each time a new trial component is added to the model, the Tucker3 analysis shown in Eq. (4) is carried out using N_i principal components. Residual shows decreasing values, starting at s_p when $N_i = 0$, until it stabilizes at a value compatible with the experimental noise, allowing to locate the correct number of components.

2.2. MCR-ALS

As it is well-known, the MCR-ALS algorithm is capable of handling second-order data sets deviating from trilinearity, *i.e.*, data in which time shifts or peak shape changes occur for analytes from sample to sample [16]. The strategy of augmenting matrices along the mode which is suspected of breaking the trilinear structure has been the choice to circumvent the latter problem. The algorithm performs a bilinear decomposition of the augmented matrix $\mathbf{D}$, according to:

$$\mathbf{D} = \mathbf{C} \times \mathbf{S}^T + \mathbf{E} \quad (5)$$

in which the rows of $\mathbf{D}$ generally contain spectra (K wavelengths) as a function of time (J times), the columns of $\mathbf{C}$ contain the time profiles of the N compounds involved in the process, the columns of $\mathbf{S}$ their related spectra, and $\mathbf{E}$ is a matrix of residuals not fitted by the model. The augmented $\mathbf{D}$ matrix is decomposed by iterative least-squares minimization of the norm of **E.** Constraining conditions (non-negativity in the spectral profiles, unimodality and non-negativity in the time profiles, correspondence among species and samples in the case of samples containing uncalibrated components) are imposed during the decomposition. $\mathbf{D}$ is built by placing one on top of another the calibration submatrices and each of the test data submatrices. The pure spectrum of each compound

should be the same in all experiments, and selective. On the other hand, the temporal profiles in the different **C** sub-matrices need not share a common shape; this is why this method is widely used to model second-order chromatographic data [1]. Finally, initialization can be performed by selection of the purest spectra based on SIMPLISMA (simple interactive self-modeling mixture analysis) [38].

In order to apply MCR-ALS to third-order data, the $\boldsymbol{X}$ ($J \times K \times L$) cube is firstly unfolded into matrices **X** ($J \times KL$), so that they could then be arranged into a bilinear augmented matrix. The general procedure followed in the present work consisted in performing several chromatographic runs, and recording the emission spectra of every one at a different excitation wavelength, across the excitation spectra of the compounds of interest. Then an EEM of size ($L \times K$), in which L and K are the number of excitation and emission wavelengths, respectively, was recorded for every elution time (gathering J EEMs). Then, data were organized for their subsequent MCR-ALS analysis. The first stage was to unfold each EEM generating a row vector of dimension ($1 \times LK$). Then, a matrix of ($J \times LK$) was created for each sample. After that, an augmented data matrix **D** of size [$J(I+1) \times LK$] was built, in which I is the number of standards and "1" represents the unknown sample under analysis.

After building the augmented matrix, MCR-ALS analysis yields an augmented concentration matrix containing the pure elution time profiles for different samples (**C**), a matrix of pure unfolded EEM profiles ($\mathbf{S}^{T}$) for the N components, and a residual matrix (**E**) containing noise and unresolved background (according to Eq. (5)). The **C** matrix contains the elution time profiles in all [$J(I+1)$] fractions for the N resolved components. The single pure unfolded EEM matrix $\mathbf{S}^{T}$ ($N \times LK$) can be reshaped as an EEM ($L \times K$) and used for the identification of the resolved components. On the other hand, the areas under the resolved time elution profiles corresponding to one sample are used for quantitative purposes. In this way, a matrix of size ($J \times N$) for every sample is obtained.

2.2.1. MCR-bands

MCR solutions are not unique and may have an unknown grade of ambiguity. In particular, intensity and rotation ambiguities can be reduced by normalization or application of constraints, respectively [39].

The MCR-BANDS method has been described to evaluate rotation ambiguity, based on the calculation of the relative contribution of every component in a mixture using a method which is evaluated using the equation:

$$f_n = \frac{\left\| \mathbf{c_n s_n^T} \right\|}{\left\| \mathbf{C S^T} \right\|} \tag{6}$$

where f_n is a scalar value which gives the relative signal contribution of a particular component to the whole signal for the mixture of N components (n=1,…N).

For every component, there will be a different set of $\mathbf{c_n}$ and $\mathbf{s_n^T}$ profiles, with different shapes due to rotation ambiguity, as well as different relative signal contribution f_n calculated with Eq. (6). The application of constraints makes only possible some of these results. It is then possible to look for maximum and minimum values of the relative contribution function for each component of the system, called respectively f_n^{max} and f_n^{min}.

After MCR modeling under a set of constraints, f_n^{max} and f_n^{min} values are calculated. In cases where rotation ambiguities are almost eliminated by the application of constraints, the profiles $\mathbf{c_n}$ and $\mathbf{s_n^T}$, and therefore f_n^{max} and f_n^{min} values, are practically constant. On the other hand, if rotation ambiguity is confirmed, the extent of rotation ambiguity can be evaluated by the difference between f_n^{max} and f_n^{min} values [40].

2.3. PARAFAC

The presently studied third-order data of size $J \times K \times L$, measured for a set of I calibration samples, can be arranged in a four-way array ($\boldsymbol{X}$), whose dimensions are [$(I+1) \times J \times K \times L$]. Provided $\boldsymbol{X}$ follows a quadrilinear PARAFAC model represented by Eq. (7), it can be written in terms of four vectors for each responsive component ($\mathbf{a}_n$, $\mathbf{b}_n$, $\mathbf{c}_n$ and $\mathbf{d}_n$) and collecting the relative concentrations [$(I+1) \times 1$] for component n, and the profiles in the three modes ($J \times 1$), ($K \times 1$) and ($L \times 1$), respectively [20].

$$x_{ijkl} = \sum_{n=1}^{N} a_{in} b_{jn} c_{kn} d_{\ln} + e_{ijkl} \tag{7}$$

The model described by the latter equation defines a decomposition of $\boldsymbol{X}$ which provides access to emission (**B**) and excitation spectral profiles (**C**), elution time profiles (**D**) and relative concentrations (**A**) of individual components in the ($I+1$) mixtures, whether they are chemically known or not. The decomposition is usually accomplished through an alternating least-squares minimization scheme [41].

PARAFAC initialization for the study of four-way arrays can be done using singular value decomposition vectors, spectral and chromatographic data which are known in advance for pure components, or by the loadings giving the best fit after small PARAFAC runs involving both singular value decomposition vectors and several sets of orthogonal random loadings, options which can be implemented in the PARAFAC package.

3. Materials and methods

3.1. Chemicals and reagents

All standards were of analytical grade. CBZ, FBZ, TBZ, CBF, CBR and NPH were provided by Sigma Aldrich (St. Louis, MO, USA). Methanol (MeOH) LC grade and acetonitrile (ACN) LC grade were obtained from Merck (Darmstadt, Germany). Dichloromethane (DM) was purchased from Cicarelli (Rosario, Argentina). Ultrapure water was obtained from a Milli-Q water purification system from Millipore (Bedford, MA, USA).

3.2. Calibration, validation and fruit juice samples

Stock standard solutions of CBZ (300.0 mg L^{-1}), TBZ (700.0 mg L^{-1}), FBZ (300.0 mg L^{-1}), CBF (510.0 mg L^{-1}), CBR (600.0 mg L^{-1}) and NPH (580.0 mg L^{-1}) were prepared by dissolving accurately weighed amounts of the pesticide standard in MeOH and maintained the solutions under refrigeration at 4 °C in the dark. More diluted solutions were prepared daily in ACN. Working standard solutions were prepared by dilution of these solutions in water.

In order to design the calibration set, the full elution time range was divided into two regions, one comprising CBZ, TBZ and FBZ and the other CBF, CBR and NPH. Two central composite designs were built for each region, obtaining a set of 15 calibration samples with the six analytes in the range of 10.0–400.0 μg L^{-1} for CBZ, 2.0–80.0 μg L^{-1} for TBZ, 0.1–1.5 μg L^{-1} for FBZ, 50.0–500.0 μg L^{-1} for CBF, 2.0–80.0 μg L^{-1} for CBR and 5.0–200.0 μg L^{-1} for NPH.

A set of 13 validation samples was prepared following the same scheme used for the calibration set, containing the six analytes in concentrations different than those used for calibration, provided by a Box-Behnken design (see Table 1).

Apples, pears and plum samples were purchased in local markets. The fruits were processed in a juice extractor. Spiked samples were obtained by diluting appropriate aliquots of standard solutions in fruit

Table 1
Predicted concentrations in validation samples using MCR-ALS, PARAFAC and U-PLS/RTL.

Analyte ($\mu g\ L^{-1}$)	Samples													REP[a]	Recovery
Method	1	2	3	4	5	6	7	8	9	10	11	12	13		$\bar{R}$ %[b]
CBZ															
Actual	175	300	300	175	50	50	175	50	175	300	300	175	50		
MCR-ALS	159	301	318	177	46	34	177	44	172	322	307	180	35	6	95
U-PLS	162	278	286	162	47	52	166	40	169	307	285	177	48	6	95
PARAFAC	162	309	321	182	48	64	177	45	190	326	318	198	49	7	104
TBZ															
Actual	35	10	35	10	60	35	60	35	10	35	60	60	10		
MCR-ALS	35	10	35	8	58	37	54	34	11	34	62	64	8	5	97
U-PLS	35	10	37	11	58	36	55	36	11	35	58	61	7	5	99
PARAFAC	35	10	36	9	58	37	55	35	11	35	61	63	8	5	99
FBZ															
Actual	0.7	0.7	1.1	0.3	0.7	1.1	0.3	0.3	1.1	0.3	0.7	1.1	0.7		
MCR-ALS	0.8	0.6	1.0	0.1	0.6	0.8	0.1	0.1	0.6	0.1	0.6	0.9	0.4	29	66
U-PLS	0.7	0.7	1.1	0.2	0.6	1.2	0.2	0.2	1.0	0.2	0.7	1.1	0.5	11	86
PARAFAC	0.7	0.6	1.0	0.1	0.6	0.8	0.1	0.1	0.7	0.1	0.6	1.0	0.4	26	67
CBF															
Actual	250	100	250	100	400	250	400	250	100	250	400	400	100		
MCR-ALS	215	110	252	108	356	230	385	241	89	248	383	407	118	7	94
U-PLS	245	101	270	92	368	245	252	239	95	228	384	392	55	8	91
PARAFAC	212	92	243	92	385	251	386	250	91	239	381	406	92	5	95
CBR															
Actual	35	60	60	35	10	10	35	10	35	60	60	35	10		
MCR-ALS	34	56	58	32	9	10	35	9	32	60	57	37	9	5	93
U-PLS	32	56	57	33	9	10	33	8	34	61	57	35	10	5	95
PARAFAC	32	55	57	32	9	9	33	9	32	58	56	34	9	6	92
NPH															
Actual	85	85	150	20	85	150	20	20	150	20	85	150	85		
MCR-ALS	83	84	137	19	77	150	18	18	138	20	81	148	66	8	92
U-PLS	83	86	140	24	78	151	19	22	135	21	79	143	65	8	98
PARAFAC	81	82	134	19	75	148	18	18	136	20	79	145	65	9	92

[a] REP, relative error prediction in %.
[b] Mean recovery.

juice. The samples were then centrifuged for 10 min at 5000 rpm. The pesticides were extracted from the supernatant by a dispersive liquid-liquid micro extraction (DLLME) procedure optimized for these samples, performed as follows: 1.0 mL of the juice sample supernatant was transferred to a 2.0 mL Eppendorf tube and 100 µL of ACN, as dispersive solvent, and 400 µL of DM, as extraction solvent, were added. The tubes were shaken for 1 minute using a vortex mixer and centrifuged for 5 min at 14,000 rpm. The lower layer (dichloromethane extract) was removed using a syringe and collected in clean test tubes. The DM was evaporated under a gentle flow of nitrogen. The final residues were reconstituted with 1.0 mL of water and vortexed for 1 min. Samples were transferred into 2 mL vials for further analysis.

3.3. HPLC-EEM procedure

The chromatographic studies were performed on an Agilent 1100 LC instrument (Agilent Technologies, Germany), equipped with degasser, quaternary pump, autosampler, oven column compartment, UV–visible diode array detector (DAD), fluorescence detector and the ChemStation software package to control the instrument, data acquisition and data analysis. The analytical column was a Zorbax Eclipse XDB-C18, 75 mm × 4.6 mm, 3.5 µm particle size (Agilent Technology, Germany).

The column temperature was controlled by setting the oven temperature at 30 °C. The mobile phase consisted in a mixture of acetonitrile and water (45:55, v/v). Samples were analyzed in isocratic mode. The complete analysis was carried out in 5 min. The flow rate was maintained at 0.80 mL min^{-1} and the acquisition frequency was 1.83 Hz. Samples were filtered through 0.45 µm nylon membrane filters before injection.

For each sample, seven chromatograms were obtained exciting at seven different excitation wavelengths (278, 283, 286, 290, 293, 296 and 305 nm) and recording the emission spectra from 305 nm to 500 nm every 1 nm. This procedure generated a data tensor of size 549 × 196 × 7. For data modeling, excitation and emission data points were reduced in order to eliminate scattering contributions. Thus, the modeling was made in the excitation range of 278–296 nm and the emission range of 335–500 nm.

3.4. Data pre-processing

The raw data obtained from the chromatographic runs were pre-processed before modeling. In order to reduce instrumental noise, a smoothing function was applied in the time direction using the Savitzky-Golay method [42]. The baseline variation between runs was corrected by digitally subtracting the blank signals from the sample data. Thus, the baseline was brought to zero for all emission and excitation wavelengths.

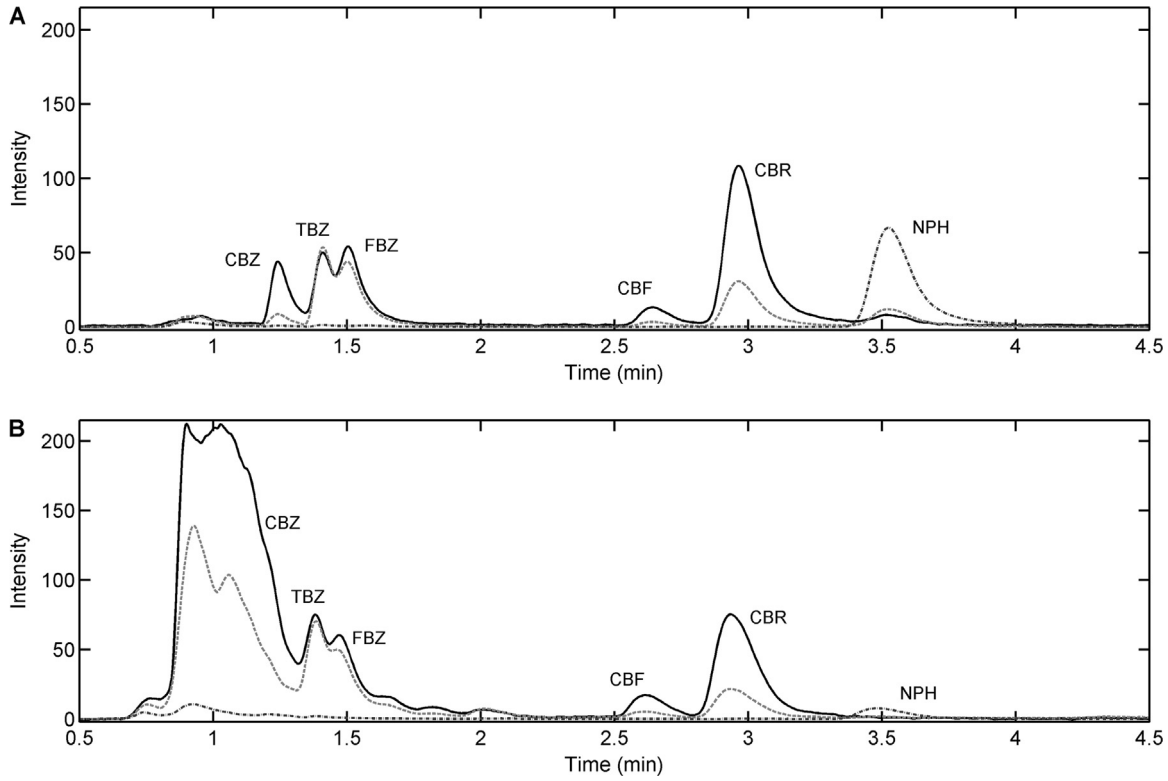

Fig. 1. (A) Chromatograms for validation sample no. 3 (Table 1) containing the six pesticides registered at λ_{ex}=283 nm and λ_{em}=325 nm (black solid line), λ_{em}=355 nm (gray dashed line) and λ_{em}=455 nm (black dash-dotted line). (B) Chromatograms for real sample no. 1 (Table 2) containing the six pesticides registered at λ_{ex}=283 nm and λ_{em}=325 nm (black solid line), λ_{em}=355 nm (gray dashed line) and λ_{em}=455 nm (black dash-dotted line).

Table 2
Predicted concentrations ($\mu g\ L^{-1}$) in fruit juice samples using U-PLS/RTL.

Fruit juice	Spiked CBZ	Found	Spiked TBZ	Found	Spiked FBZ	Found
Apple	0	26	0	5.0	0	ND
	30	55 (97)	10	13.4 (84)	0.30	0.21 (70)
Pear	0	36	0	ND	0	ND
	150	146 (73)	40	39 (97)	0.80	0.78 (97)
Plum	0	13	0	3.9	0	0.1
	150	83 (48)	40	24 (51)	0.80	0.6 (63)
	CBF		CBR		NPH	
Apple	0	ND	0	ND	0	ND
	100	81 (81)	10	10 (100)	10	11 (110)
Pear	0	ND	0	ND	0	NR
	250	211 (85)	40	34 (88)	95	NR
Plum	0	ND	0	ND	0	NR
	250	263 (105)	40	43 (107)	95	NR

NR: samples that could not be resolved.
Between parenthesis: recoveries (%), computed as: 100 × (Predicted value in the spiked sample − Predicted value in non-spiked sample)/Nominal spiked value.

3.5. Software

The ChemStation software (Agilent Technologies, Germany) was employed for LC instrument control. All employed algorithms were implemented in MATLAB 7.6 [43]. Those for applying MCR-ALS are available on the Internet at http://www.mcrals.info/. A useful interface for data input and parameters setting written by Olivieri et al. [44], which can be downloaded from www.iquir-conicet.gov.ar/descargas/mvc3.rar, was employed to PARAFAC, MCR-ALS and U-PLS/RTL implementation.

4. Results and discussion

4.1. Third-order data generation

Fig. 1A and B shows chromatograms for validation sample no. 3 (Table 1) containing the six pesticides registered at λ_{ex}=283 nm and λ_{em}=325, 355 and 455 nm, and chromatograms for apple juice real sample (Table 2) at the same conditions. These three emission wavelengths were chosen in order to show that wavelength selection is not a trivial operation. As can be appreciated, the six analytes cannot be completely separated by the chromatographic method, and, additionally, the real sample contains a large number of unexpected constituents. On the other hand, a single chromatographic run only requires 4 min to be carried out. This latter fact is of paramount significance because the third-order data generation procedure implemented herein requires seven chromatographic runs per sample, as was commented above.

Fig. 2 shows excitation and emission spectra of CBZ, TBZ, FBZ, CBF, CBR and NPH obtained in a spectrofluorimeter by measuring pure standard solutions of each pesticide. Interestingly, this figure demonstrates that selectivity can be improved taking advantage of the differences in the excitation spectra, instead of using a single excitation wavelength to generate the emission spectra.

Fig. 3 shows four contour plots, each one corresponding to chromatogram-emission spectra matrices recorded at the following excitation wavelengths: 278, 286, 293, 305 nm for validation sample no. 1 (Table 1). A visual inspection of these four contour plots makes evident the large amount of information that can be obtained by using the described data generating procedure.

First, it is worth mentioning the importance of working with second-order data, considering that the selection of one emission and one excitation wavelength would restrict the number of compounds that can be detected in a chromatographic run, or

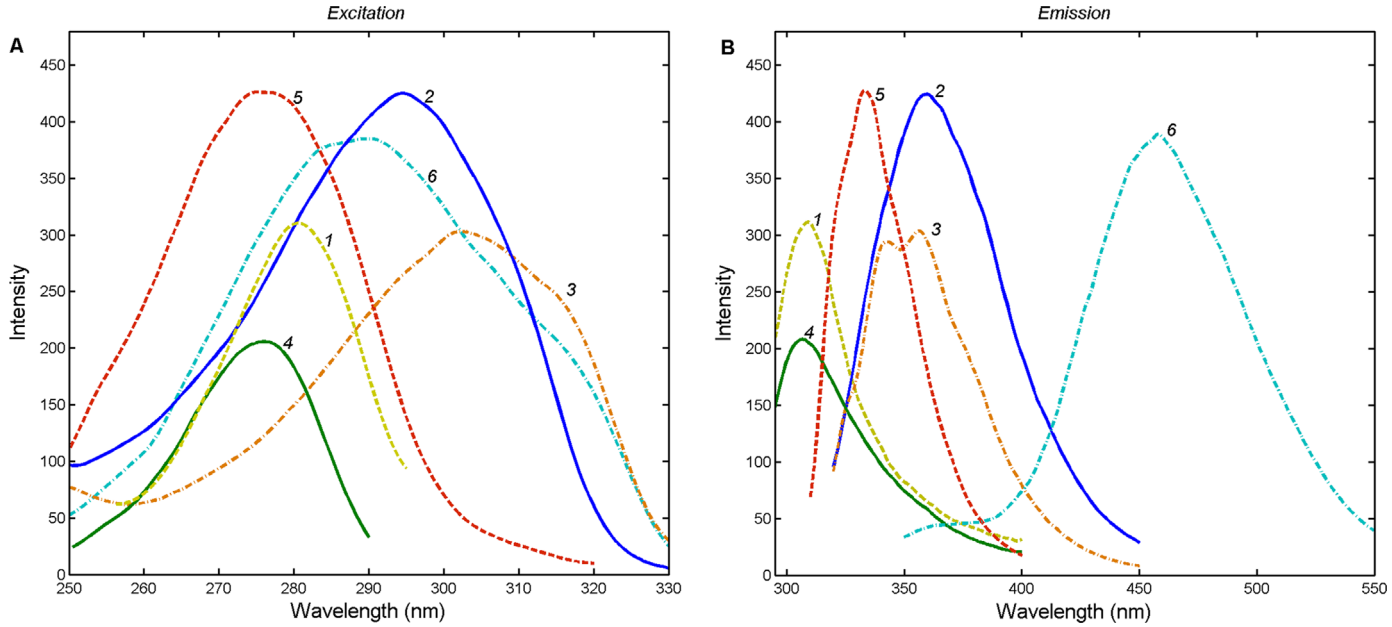

Fig. 2. Excitation (A) and emission (B) spectra for the six pesticides. 1-CBZ: yellow dashed line, 2-TBZ: blue solid line, 3-FBZ: orange dash-dotted line, 4-CBF: green solid line, 5-CBR: red dashed line and 6-NPH: cyan dash-dotted line. Conditions: (A) excitation spectra of CBZ (λ_{em}=310 nm), TBZ (λ_{em}=360 nm), FBZ (λ_{em}=355 nm), CBF (λ_{em}=307 nm), CBR (λ_{em}=335 nm) and NPH (λ_{em}=458 nm). (B) Emission spectra of CBZ (λ_{ex}=383 nm), TBZ (λ_{ex}=296 nm), FBZ (λ_{ex}=304 nm), CBF (λ_{ex}=278 nm), CBR (λ_{ex}=278 nm) and NPH (λ_{ex}=290 nm). Concentrations: CBZ: 200 mg L^{-1}, TBZ: 100 mg L^{-1}, FBZ: 10 mg L^{-1}, CBF: 200 mg L^{-1}, CBR: 100 mg L^{-1}, NPH: 100 mg L^{-1}. (For interpretation of the references to color in this figure legend, the reader is referred to the web version of this article.)

would significantly reduce the sensitivity of the method. However, recording the emission spectra is probably not sufficient as the analytes present different excitation maxima and this is evidenced in Figs. 1 and 3. In going from one excitation wavelength to another, the signals of some analytes decrease as the signals of others become stronger. For instance, the signal of CBF and CBR, which elute at 2.7 and 3.0 minute, respectively, and have the maximum excitation intensity at 278 nm, is evidently favored in the first contour plot (λ_{ex}=278 nm), and gradually decreases until the last one (λ_{ex}=305 nm), in which no signal of them is detected. The opposite behavior is observed for TBZ (1.4 min) and FBZ (1.6 min), since the signal increases from the first contour plot to the last one, in agreement with their excitation maxima (296 nm and 305 nm, respectively).

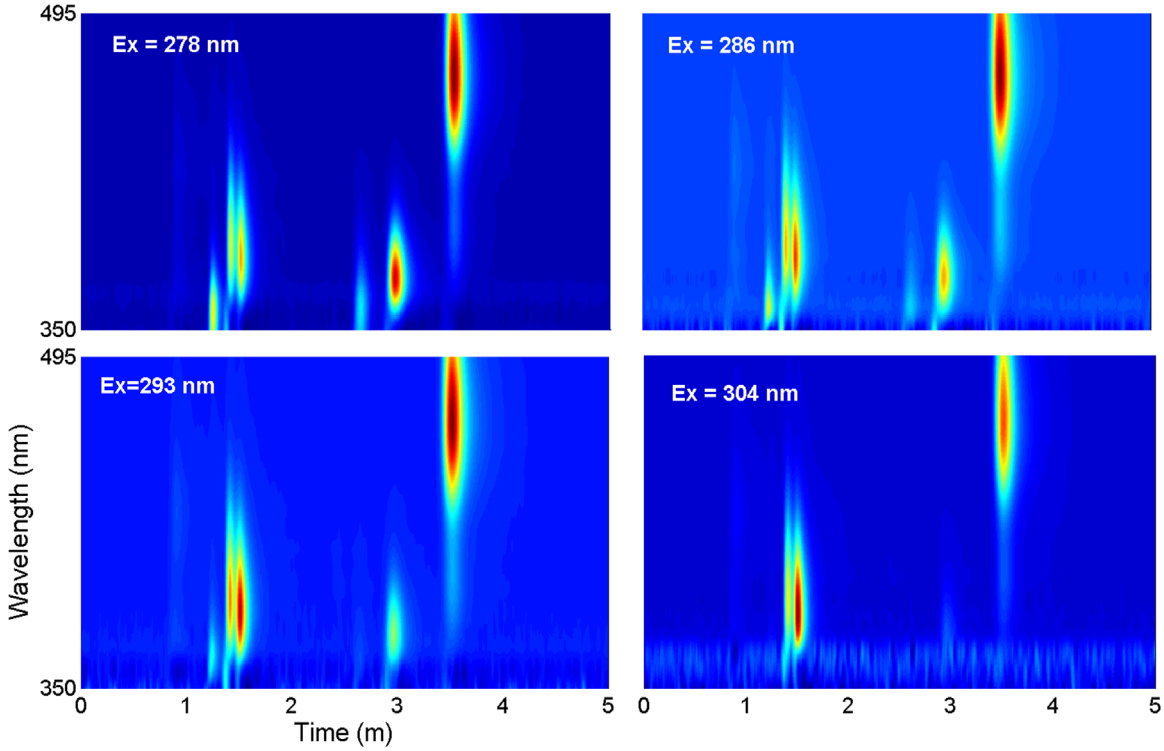

Fig. 3. Contour plots, each one corresponding to chromatogram-emission spectra matrices recorded at four excitation wavelengths for validation sample no. 1 (Table 1).

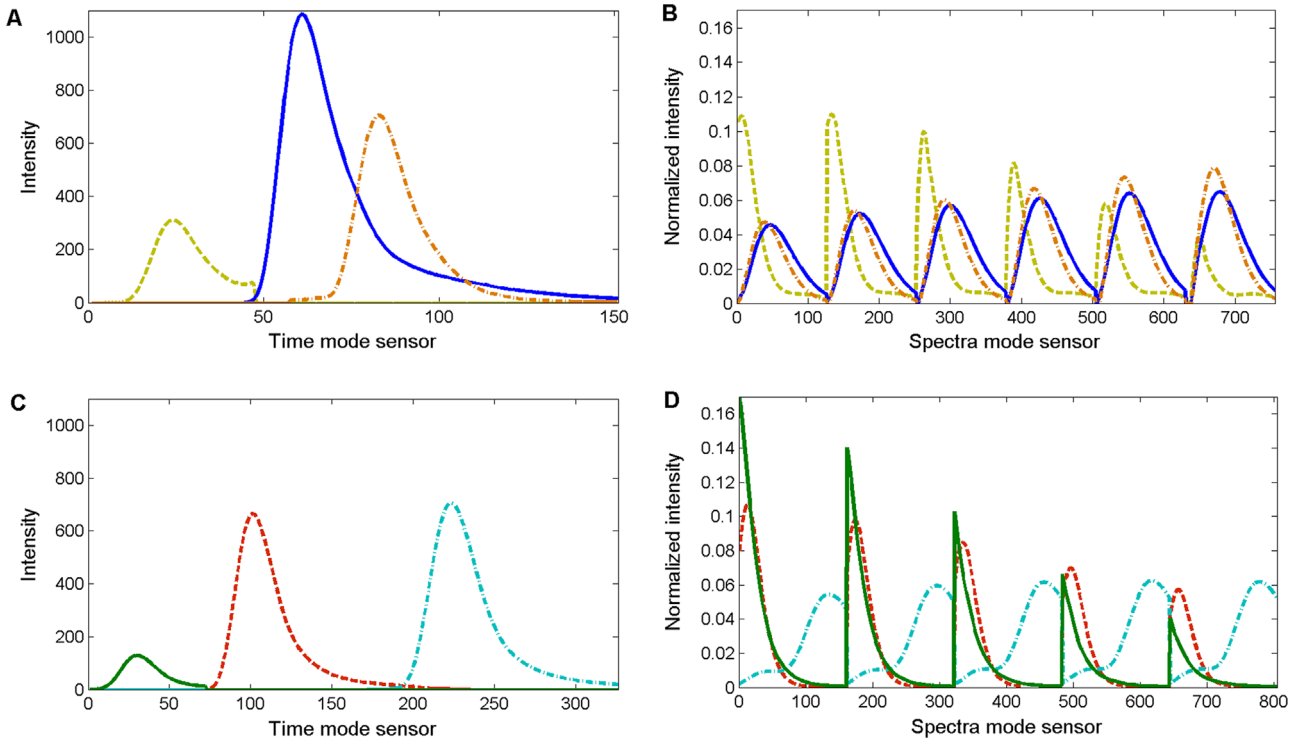

Fig. 4. Temporal (A–C) and spectral (B–D) profiles retrieved by MCR-ALS analysis for validation sample no. 6. (A and B) CBZ: yellow dashed line, TBZ: blue solid line and FBZ: orange dash-dotted line; (C and D) CBF: green solid line, CBR: red dashed line and NPH: cyan dash-dotted line. (For interpretation of the references to color in this figure legend, the reader is referred to the web version of this article.)

4.2. MCR-ALS modeling of second- and third-order data

In order to quantify the six analytes in the thirteen validation samples, two **D** augmented matrices were built by appending: (a) the second-order calibration data matrices consisting in time-emission spectra recorded at λ_{ex}=283 nm split into two regions: region I (1.1–1.8 min) and region II (2.5–4.0 min); and (b) the third-order calibration data matrices (time-unfolded EEM, equally split into two regions as for second-order data).

Augmented matrices were built appending one validation sample plus the fifteen calibration sample data. During the ALS optimization, the following constraints were applied to get unique and physically meaningful solutions: (a) non-negativity in the concentration and spectral profiles, (b) unimodality in the concentration profiles, and (c) trilinearity.

In addition, based on the knowledge of the system under study, three compounds, in each time region, were used to build the spectral initial estimations using the simple-to-use interactive self-modeling mixture analysis (SIMPLISMA) methodology [38]. After MCR-ALS decomposition of **D** matrices according to Eq. (5), the concentration information contained in both **C** matrices was used to construct pseudounivariate graphs by plotting the analyte concentration scores against the nominal analyte concentrations. Table 1 shows the results for third-order data and Table 1S (see Supplementary material) for second-order data.

As can be seen in Table 1, MCR-ALS modeling furnishes good results, with relative error predictions (REP%) of 5–7, except for FBZ (REP=29%). When going from second- to third-order data the prediction ability improves for the six analytes, although the predictions for FBZ were still not satisfactory.

In Fig. 4, the profiles retrieved by MCR-ALS after decomposing the augmented **D** matrix for third-order data are shown. As can be seen, decomposition of **D** furnishes the temporal and spectral profiles (concatenated emission spectra corresponding to each

Table 3
Effect of constraints on rotation ambiguity in MCR-ALS.

Constraints[a]	f	Region I			Region II		
		Component 1	Component 2	Component 3	Component 1	Component 2	Component 3
1,2,3	f^{max}	0.284	0.844	0.494	0.413	0.684	0.993
	f^{ini}	0.231	0.781	0.457	0.642	0.757	0.119
	f^{min}	0.184	0.460	0.207	0.388	0.542	0.609
	$\mathbf{f^{max}-f^{min}}$	0.100	0.384	0.287	0.025	0.142	0.384
1,2,3,4	f^{max}	0.229	0.799	0.385	0.643	0.756	0.119
	f^{ini}	0.229	0.799	0.385	0.643	0.756	0.119
	f^{min}	0.229	0.799	0.385	0.643	0.756	0.119
	$\mathbf{f^{max}-f^{min}}$	0.000	0.000	0.000	0.000	0.000	0.000

f^{max} – f^{min} corresponds to the difference between f^{max} and f^{min} values.

[a] Constraints: 1 normalization; 2 non-negativity; 3 unimodality; 4 trilinearity.

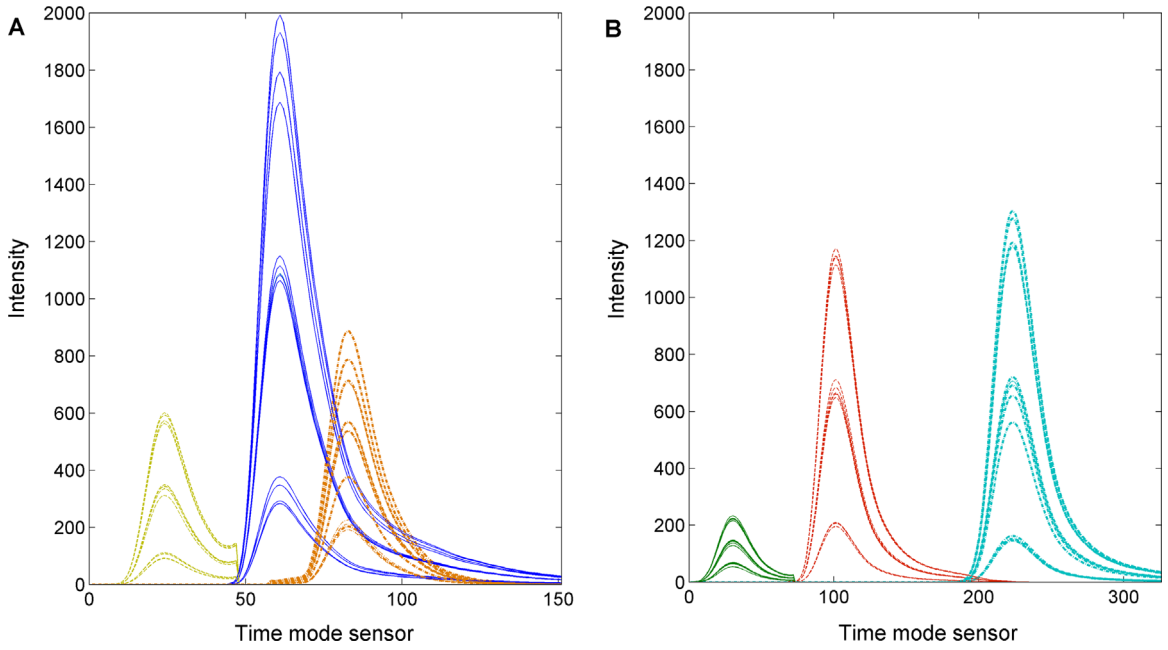

Fig. 5. Overlapped time profiles of 13 validation samples. (A) CBZ: yellow dashed line, TBZ: blue solid line and FBZ: orange dash-dotted line; (B) CBF: green solid line, CBR: red dashed line and NPH: cyan dash-dotted line. (For interpretation of the references to color in this figure legend, the reader is referred to the web version of this article.)

excitation wavelength) for every compound in region I (Fig. 4A and B) and in region II (Fig. 4 C and D). Comparison of the results with the pure spectra allows affirming that the modeling results were satisfactory and the spectra profiles retrieved are in agreement with the spectra of pure analytes.

In addition, rotational ambiguity was evaluated considering different types of constraints. In Table 3, a summary of the results obtained using the MCR Bands program is shown [40]. The values of f_n^{min}, f_n^{inic}, f_n^{max} and the difference between f_n^{max} and f_n^{min} are given for every component when non-negativity and unimodality constraints were used, and when the trilinearity constraint was applied in addition to non-negativity and unimodality. As can be appreciated, the trilinearity constraint completely eliminates the rotation ambiguity, as proved by f_n^{min} and f_n^{max} values, and their comparison with those corresponding to f_n^{inic}.

Fig. 5, which shows the retrieved time profiles for all the validation samples, lets us arrive to an interesting observation: no major peak time shifts occurred among samples. This fact conducts us to the conclusion that there is no trilinearity loss, and consequently, that other algorithms such as PARAFAC and U-PLS/RTL could be successfully applied.

Table 4
Analytical figures of merit for the application of PARAFAC, MCR-ALS and U-PLS methods to the modeling of second- and third-order data for validation and fruit juice samples.[a]

	CBZ			**TBZ**			**FBZ**		
	MCR-ALS	U-PLS	PARAFAC	MCR-ALS	U-PLS	PARAFAC	MCR-ALS	U-PLS	PARAFAC
Validation samples									
Sensitivity	2/3	8/20	5/7	10/25	30/89	38/110	220/710	1300/3900	1100/3100
$[\gamma^{-1}]$[b]	1/0.4	0.2/0.1	0.1/0.3	0.3/0.1	0.05/0.02	0.01/0.01	0.01/0.003	0.001/0.0004	0.0004/0.0005
LOD ($\mu g\ L^{-1}$)[c]	24/32.0	4.7/2.1	18/18	4.4/8.7	1.2/0.6	6.3/5.5	0.4/0.4	0.04/0.02	0.3/0.3
Fruit juice									
Sensitivity	–	10	–	–	34	–	–	1380	–
$[\gamma^{-1}]$[b]	–	0.2	–	–	0.05	–	–	0.001	–
LOD ($\mu g\ L^{-1}$)[c]	–	30	–	–	7.0	–	–	0.07	–

	CBF			**CBR**			**NPH**		
	MCR-ALS	U-PLS	PARAFAC	MCR-ALS	U-PLS	PARAFAC	MCR-ALS	U-PLS	PARAFAC
Validation samples									
Sensitivity	0.5/0.6	5/13	1.4/3	14/18	38/100	48/95	9/20	12/34	20/45
$[\gamma^{-1}]$[b]	2/1	0.3/0.1	0.4/0.4	0.08/0.04	0.04/0.02	0.01/0.01	0.1/0.03	0.1/0.05	0.03/0.02
LOD ($\mu g\ L^{-1}$)[c]	100/110	12.2/4.6	59/4.7	2.4/2.8	0.9/0.4	1.8/1.9	12/12	4.9/2.4	11/11
Fruit juice									
Sensitivity	–	6	–	–	41	–	–	11	
$[\gamma^{-1}]$[b]	–	0.1	–	–	0.02	–	–	0.07	
LOD ($\mu g\ L^{-1}$)[c]	–	20	–	–	3.1	–	–	7.3	

Figures of merit were not computed for MCR-ALS and PARAFAC in fruit juice samples.

[a] Second-order/third-order.
[b] Inverse of analytical sensitivity
[c] LOD: Limit of detection.

4.3. PARAFAC modeling of second- and third-order data

The thirteen validation samples (Table 1) were investigated with PARAFAC. In order to model the data with this algorithm, the first step is the assessment of the correct number of sample constituents. This number is determined based on several different criteria, such as previous knowledge of the system, variance explained by the model and core consistency diagnosis (CORCONDIA), proposed by Bro and Kiers [45]. For the latter criteria, when the selected number is bigger than the correct factor number, the core consistency is close to zero or even negative. When the selected number is equal to or smaller than the correct number, the core consistency is close to one. However, it is not rare that different diagnostics point to different number of components. Considering this, the number of components was six, with an explained variance of 99.1%, which is in agreement with the known number of compounds present in the calibration and validation sets.

Different models were built for each analyte. For modeling both second- and third-order data, matrices or cubes corresponding to the calibration samples were stacked with the one corresponding to the target sample. Decompositions were performed applying the following constraints: unimodality in the time mode and non-negativity in the others.

After PARAFAC decomposition of the three- or four-way arrays, the concentration information contained in the score matrices was used to build the pseudounivariate graph by plotting the analyte concentration scores against the nominal analyte concentrations. Predictions are depicted in Table 1 for third-order data and Table 1S for second-order data, while figures of merit are shown in Table 4 and discussed below.

4.4. U-PLS/RTL modeling of second- and third-order data

U-PLS was applied selecting the number of latent variables by the well-known leave-one-sample-out cross-validation procedure [37]. Thus, the optimum number of factors was estimated by calculating the ratios $F(A)=PRESS(A<A^*)/PRESS(A^*)$, where $PRESS=\Sigma(y_{i,act}-y_{i,pred})^2$, A is a trial number of factors and A^* corresponds to the minimum PRESS, and selecting the number of factors leading to a 75%-less probability that $F>1$. Since the present study was carried out with six pesticides A was equal to 6.

Table 1 shows the prediction results for MCR-ALS, U-PLS/RTL and PARAFAC modeling of the validation samples for third order data. As can be appreciated, the algorithms achieved similar error predictions (5-9%) for five of the six analytes. However, there is an evident difference in their prediction ability for the analyte FBZ. U-PLS/RTL attained a REP%=11, while for MCR-ALS and PARAFAC it was 29 and 26, respectively. This significant improvement in prediction for FBZ can be attributed to the higher sensitivity reached by U-PLS/RTL, with a limit of detection 10-time lower than those for both PARAFAC and MCR-ALS (see below). On the other hand, it has been proven the higher ability of this latent-variable structured algorithm when modeling highly collinear systems [46].

The statistical comparison of the prediction results presented in Table 1 (and those obtained for second-order data modeling shown in the Table 1S of Supplementary material) was made via the bivariate least squares (BLS) regression method and the elliptic joint confidence region (EJCR) test [47]. The EJCR plots of the slopes and the intercepts are shown in Fig. 6A–C for second-order data, and Fig. 6D–F for third-order data modeling. A visual inspection of the six figures allows arriving to an interesting conclusion: the elliptical domains obtained with all the data and the algorithms applied to the six analytes only contain the theoretically predicted value of the slope (1) and the intercept (0) for

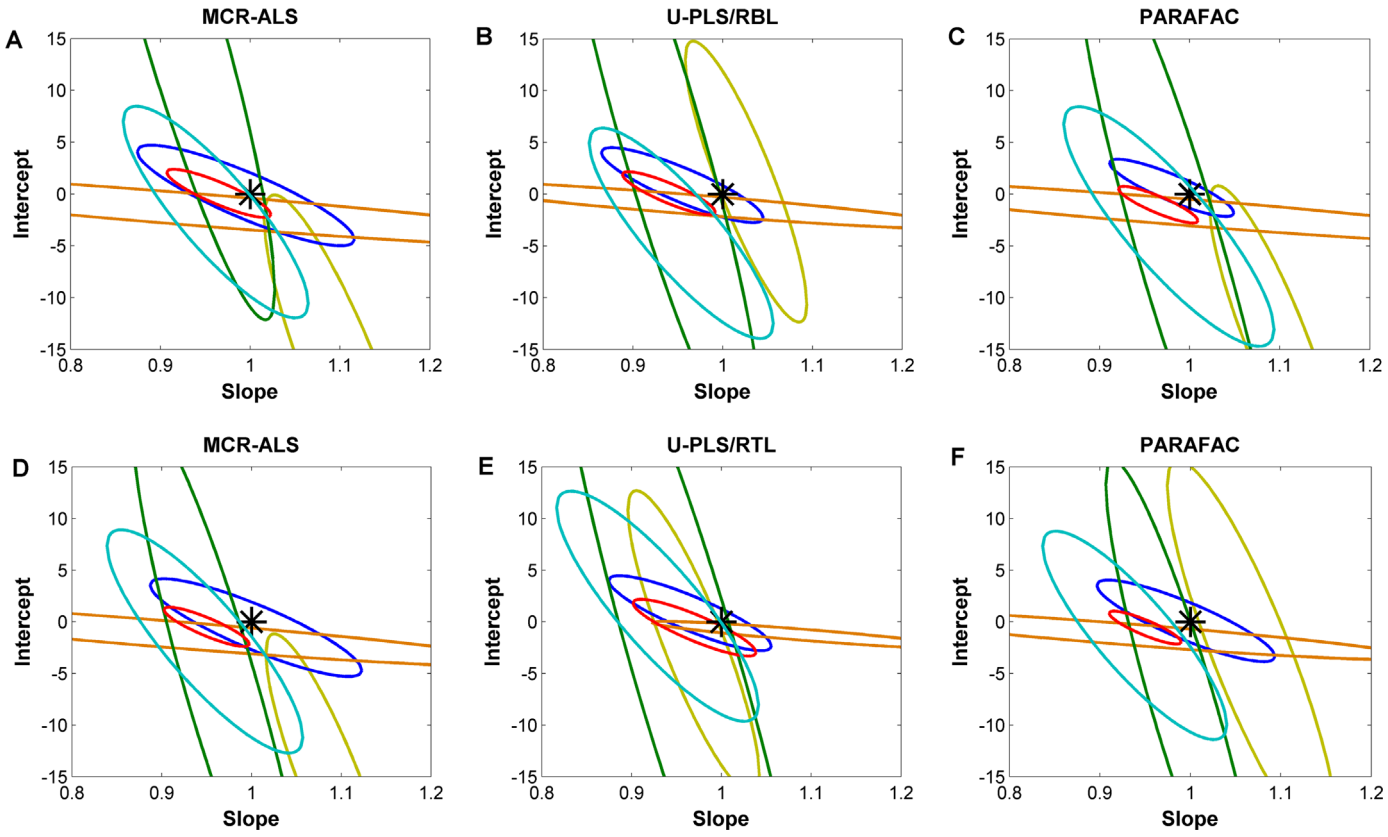

Fig. 6. EJCR plots of the slopes and the intercepts for second-order data (A–C), and for third-order data modeling (Fig. 6D–F). For CBZ, TBZ, FBZ, CBF, CBR, NPH in yellow, blue, orange, green, red and cyan line, respectively. (For interpretation of the references to color in this figure legend, the reader is referred to the web version of this article.)

U-PLS/RTL (Fig. 6E). This fact is indicative of the better performance of the latter algorithm, and consequently, fruit juice samples were analyzed by implementing U-PLS/RTL.

4.5. Quantitative results obtained in fruit juice samples

In order to evaluate the performance of U-PLS/RTL in terms of its predictive ability, predictions obtained for the fruit juice samples without and with spiked analytes are presented in Table 2. A matrix effect was observed in the analysis of these samples, probably due to the presence of a large number of components in the extracting liquid. Thus, quantitation was performed by the standard addition calibration method, which involved spiking three levels of each standard to samples without and with the target analytes.

The number of factors was estimated using the leave-one-sample-out cross-validation procedure. The number of latent variable was six for apple and five for the other two samples, because NPH was affected by matrix effect in pear and plum and could not be quantified. Due to the presence of uncalibrated compounds, RTL was applied to achieve the second order advantage. Two interferents in the RTL procedure were necessary to stabilize the final residuals.

As can be appreciated in Table 2, the best results were obtained for CBF and CBR (recoveries ranged between 85% and 113%). It should be noted that both analytes are present in the second region, and reach the better chromatographic separation (see Fig. 1). According to the latter comment, it would be expected the same behavior for NPH. But, regrettably, NPH was the most affected analyte by the matrix effect, especially in pear and plum samples. Consequently, it could not be quantified in these particular samples.

Another interesting fact that deserves to be commented is the presence of CBZ and TBZ in the three analyzed fruit juice, and FBZ in plum juice. This latter analyte in a very low concentration (0.1 $\mu g\ L^{-1}$), but over the LOD computed for U-PLS/RTL of 0.02 $\mu g\ L^{-1}$ (see below).

4.6. Analytical figures of merit

Figures of merit were calculated in order to evaluate the applicability of the proposed method. Sensitivity (SEN) can be considered as one of the most relevant figures of merit in the field of analytical chemistry due to the fact that it is a decisive factor in estimating others, such as limit of detection (LOD) and limit of quantitation (LOQ). SEN can be defined as the variation in net response for a given change in analyte concentration.

Very recently, expressions for multi-way calibration methods, such as MCR-ALS [48] and U-PLS/RBL or RTL [49], were derived based on the concept of input and output noise in a given system (SEN measures the ratio of output noise to input noise). These expressions were used to compute the figures of merit presented in Table 4. It should be remarked the enhancement in SEN and the reduction in LOD and LOQ when going from second- to third-order data for the same algorithm. This fact has been pointed out by Allegrini and Olivieri [49], and encourages increased research on the field of generation of new high-order data.

Comparing the results obtained in the present work with those presented in reported papers, an improvement in LOD and LOQ, as well as in sensitivity, is observed for some of the pesticides. The limits found are quite varied, depending on the method employed. The LODs reported in the literature are between 0.6 and 65 $\mu g\ L^{-1}$ for CBZ, 0.02–0.30 $\mu g\ L^{-1}$ for FBZ, 0.3–4.5 $\mu g\ L^{-1}$ for TBZ, 0.13 $\mu g\ L^{-1}$–4.0 $\mu g\ L^{-1}$ for CBF, 0.8–30 $\mu g\ L^{-1}$ for CBR, and 2–18 $\mu g\ L^{-1}$ for NPH. A comparison let us conclude that the results obtained by the method presented in this work can be considered satisfactory and, in some cases, better than those obtained by other methods [25,27,28, 29,31,35]. It is worth mentioning that, apart from achieving desired limits of detection, the method described is suitable for quantifying five analytes in a reasonable analysis time, even in the presence of interferents, which becomes especially important when dealing with complex matrices such as fruits juice.

5. Conclusions

The acquisition and the proper modeling of four-way data acquired by following excitation–emission fluorescence matrices at different elution times in a fast HPLC procedure can become a way to improve the analytical ability when analyzing complex samples.

The modeling of the data considered in the present work resulted more convenient with U-PLS/RTL than with the other two well-known algorithms: PARAFAC and MCR-ALS. Thus, it could be concluded that when no peak time shifts occurred among samples and there is high colinearity in one mode, the latent-variable structured algorithm is capable of better handle the need of high sensitivity for the analysis of one of the analytes. More studies are needed to fully understand the structure of four-way arrays and to develop analytical methods for increasingly complex samples.

Acknowledgements

The authors are grateful to Universidad Nacional del Litoral (Projects CAI+D 2011 Nos. 11-11 and 11-7), to CONICET (Consejo Nacional de Investigaciones Científicas y Técnicas, Project PIP-2012 No. 455) and to ANPCyT (Agencia Nacional de Promoción Científica y Tecnológica, Project PICT 2014–0347) for financial support. M.M. thanks CONICET for her fellowship. Brazilian authors are grateful to CNPq by scholarship, research fellowships and for financial support (MCTI/CNPq no. 19/2011).

Appendix A. Supplementary material

Supplementary data associated with this article can be found in the online version at http://doi:10.1016/j.talanta.2016.03.078.

References

[1] G.M. Escandar, H.C. Goicoechea, A. Muñoz de la Peña, A.C. Olivieri, Second- and higher-order data generation and calibration: a tutorial, Anal. Chim. Acta 806 (2014) 8–26.
[2] H.C. Goicoechea, M.J. Culzoni, M.D. Gil García, M. Martínez Galera, Chemometric strategies for enhancing the chromatographic methodologies with second-order data analysis of compounds when peaks are overlapped, Talanta 83 (2011) 1098–1107.
[3] M. Vosough, M. Rashvand, H.M. Esfahani, K. Kargosha, A. Salemi, Direct analysis of six antibiotics in wastewater samples using rapid high-performance liquid chromatography coupled with diode array detector: a chemometric study towards green analytical chemistry, Talanta 135 (2015) 7–17.
[4] M. Martinez Galera, M.D. Gil García, M.J. Culzoni, H.C. Goicoechea, Determination of pharmaceuticals in river water by column switching of large sample volumes and liquid chromatography–diode array detection, assisted by chemometrics: an integrated approach to green analytical methodologies, J. Chromatogr. A 1217 (2010) 2042–2049.
[5] A. Mancha de Llanos, M.M. De Zan, M.J. Culzoni, A. Espinosa Mansilla, F. Cañada Cañada, A. Muñoz de la Peña, H.C. Goicoechea, Determination of marker pteridines in urine by HPLC with fluorimetric detection and second-order multivariate calibration using MCR-ALS, Anal. Bioanal. Chem. 399 (2011) 2123–2135.
[6] M.J. Culzoni, A. Mancha de Llanos, M.M. De Zan, A. Espinosa Mansilla, F. Cañada Cañada, A. Muñoz de la Peña, H.C. Goicoechea, Enhanced MCR-ALS modeling of HPLC with fast scan fluorimetric detection second-order data for quantitation of metabolic disorder marker pteridines in urine, Talanta 85 (2011) 2368–2374.
[7] F. Cañada Cañada, J.A. Arancibia, G.M. Escandar, G.A. Ibañez, A. Espinosa Mansilla, A. Muñoz de la Peña, A.C. Olivieri, Second-order multivariate

calibration procedures applied to high-performance liquid chromatography coupled to fast-scanning fluorescence detection for the determination of fluoroquinolones, J. Chromatogr. A 1216 (2009) 4868–4876.
[8] S.A. Bortolato, J.A. Arancibia, G.M. Escandar, Non-trilinear chromatographic time retention − fluorescence emission data coupled to chemometric algorithms for the simultaneous determination of 10 polycyclic aromatic hydrocarbons in the presence of interferences, Anal. Chem. 81 (2009) 8074–8084.
[9] M. Vosough, M. Bayat, A. Salemi, Matrix-free analysis of aflatoxins in pistachio nuts using parallel factor modeling of liquid chromatography diode-array detection data, Anal. Chim. Acta 663 (2010) 11–18.
[10] X.-H. Zhang, H.-L. Wu, J.-Y. Wang, D.-Z. Tu, C. Kang, J. Zhao, Y. Chen, X.-X. Miu, R.-Q. Yu., Fast HPLC-DAD quantification of nine polyphenols in honey by using second-order calibration method based on trilinear decomposition algorithm, Food Chem. 138 (2013) 62–69.
[11] H. Parastar, J.R. Radovic, M. Jalali-Heravi, S. Diez, J.M. Bayona, R. Tauler., Resolution and quantification of complex mixtures of polycyclic aromatic hydrocarbons in heavy fuel oil sample by means of gc × gc-tofms combined to multivariate curve resolution, Anal. Chem. 83 (2011) 9289–9297.
[12] V.A. Lozano, A. Muñoz de la Peña, I. Durán-Merás, A. Espinosa Mansilla, G. M. Escandar, Four-way multivariate calibration using ultra-fast high-performance liquid chromatography with fluorescence excitation–emission detection. Application to the direct analysis of chlorophylls a and b and pheophytins a and b in olive oils, Chemom. Intell. Lab. Syst. 125 (2013) 121–131.
[13] M. Alcaráz, G. Siano, M. Culzoni, A. Muñoz de la Peña, H.C. Goicoechea, Modeling four and three-way fast high-performance liquid chromatography with fluorescence detection data for quantitation of fluoroquinolones in water samples, Anal. Chim. Acta 809 (2014) 37–46.
[14] E. Bezemer, S.C. Rutan., Analysis of three- and four-way data using multivariate curve resolution-alternating least squares with global multi-way kinetic fitting, Chemom. Intell. Labo. Syst. 81 (2006) 82–93.
[15] X.-D. Qing, H.-L. Wu, X.-H. Zhang, Y. Li, H.-W. Gu, R.-Q. Yu., A novel fourth-order calibration method based on alternating quinquelinear decomposition algorithm for processing high performance liquid chromatography–diode array detection– kinetic-pH data of naptalam hydrolysis, Anal. Chim. Acta 861 (2015) 12–24.
[16] R. Tauler, Multivariate curve resolution applied to second order data, Chemom. Intell. Lab. Syst. 30 (1995) 133–146.
[17] H.P. Bailey, S.C. Rutan, Chemometric resolution and quantification of four-way data arising from comprehensive 2d-LC-DAD analysis of human urine, Chemom. Intell. Lab. Syst. 106 (2011) 131–141.
[18] J.A. Arancibia, A.C. Olivieri, D. Bohoyo Gil, A. Espinosa Mansilla, I. Durán Merás, A. Muñoz de la Peña, Trilinear least-squares and unfolded-PLS coupled to residual trilinearization: new chemometric tools for the analysis of four-way instrumental data, Chemom. Intell. Lab. Syst. 80 (2006) 77–86.
[19] P.C. Damiani, I. Durán Merás, A.G. García Reiriz, A. Jimenez Girón, A. Muñoz de la Peña, A.C. Olivieri., Multiway partial least-squares coupled to residual trilinearization: a genuine multidimensional tool for the study of third-order data. simultaneous analysis of procaine and its metabolite p-aminobenzoic acid in equine serum, Anal. Chem. 76 (2007) 6949–6958.
[20] C.M. Andersen, R. Bro, Practical aspects of PARAFAC modeling of fluorescence excitation-emission data, J. Chemom. 17 (2003) 200–215.
[21] S.A. Bortolato, V.A. Lozano, A. Muñoz de la Peña, A.C. Olivieri, Novel augmented parallel factor model for four-way calibration of high-performance liquid chromatography-fluorescence excitation-emission data, Chemom. Intell. Lab. Syst. 141 (2015) 1–11.
[22] S. Topuz, G. Özhan, B. Alpertunga, Simultaneous determination of various pesticides in fruit juices by HPLC-DAD, Food Control 16 (2005) 87–92.
[23] European Commission, ⟨http://ec.europa.eu/⟩.
[24] U.S. Department of Health & Human Services. U.S. Food and Drug Administration, ⟨http://www.fda.gov/⟩.
[25] P. Santa-Cruz, A. García-Reiriz, Application of third-order multivariate calibration algorithms to the determination of carbaryl, naphthol and propoxur by kinetic spectroscopic measurements, Talanta 128 (2014) 450–459.
[26] L. Rubio, L.A. Sarabia, M.C. Ortiz, Standard addition method based on four-way PARAFAC decomposition to solve the matrix interferences in the determination of carbamate pesticides in lettuce using excitation–emission fluorescence data, Talanta 138 (2015) 86–99.
[27] M.J. Rodríguez-Cuesta, R. Boqué, F.X. Rius, D.P. Zamora, M. Martínez Galera, A. Garrido Frenich, Determination of carbendazim, fuberidazole and thiabendazole by three-dimensional excitation–emission matrix fluorescence and parallel factor analysis, Anal. Chim. Acta 491 (2003) 47–56.
[28] V. Boeris, J.A. Arancibia, A.C. Olivieri, Determination of five pesticides in juice, fruit and vegetable samples by means of liquid chromatography combined with multivariate curve resolution, Anal. Chim. Acta 814 (2014) 23–30.
[29] M. Arsenio-Ramos, J. Hernández-Borges, T.M. Borges-Miquel, M.A. Rodríguez-Delgado, Ionic liquid-dispersive liquid–liquid microextraction for the simultaneous determination of pesticides and metabolites in soils using high-performance liquid chromatography and fluorescence detection, J. Chromatogr. A 1218 (2011) 4808–4816.
[30] Q. Subhani, Z. Huang, Z. Zhu, Y. Zhu, Simultaneous determination of imidacloprid and carbendazim in water samples by ion chromatography with fluorescence detector and post-column photochemical reactor, Talanta 116 (2013) 127–132.
[31] C. Raeppel, M. Nief, M. Fabritius, L. Racault, B.M. Appenzeller, M. Millet, Simultaneous analysis of pesticides from different chemical classes by using a derivatisation step and gas chromatography–mass spectrometry, J. Chormatogr. A 1218 (2011) 8123–8129.
[32] J. Wang, Z. Du, W. Yu, S. Qu, Detection of seven pesticides in cucumbers using hollow fibre-based liquid-phase microextraction and ultra-high pressure liquid chromatography coupled to tandem mass spectrometry, J. Chormatogr. A 1247 (2012) 10–17.
[33] E.Y. Yang, H.S. Shin, Trace level determinations of carbamate pesticides in surface water by gas chromatography–mass spectrometry after derivatization with 9-xanthydrol, J. Chromatogr. A 1305 (2013) 328–332.
[34] D. Moreno-González, J.F. Huertas-Pérez, A.M. García-Campaña, L. Gámiz-García, Vortex-assisted surfactant-enhanced emulsification liquid–liquid microextraction for the determination of carbamates in juices by micellar electrokinetic chromatography tandem mass spectrometry, Talanta 139 (2015) 174–180.
[35] M. Wang, J. Huang, M. Wang, D. Zhang, J. Chen, Electrochemical nonenzymatic sensor based on CoO decorated reduced graphene oxide for the simultaneous determination of carbofuran and carbaryl in fruits and vegetables, Food Chem. 151 (2014) 191–197.
[36] S. Wold, P. Geladi, K. Esbensen, J. Øhman., Multi-way principal components-and PLS-analysis, J. Chemom. 1 (1987) 41–56.
[37] D.M. Haaland, E.V. Thomas, Partial least-squares methods for spectral analyses. 1. Relation to other quantitative calibration methods and the extraction of qualitative information, Anal. Chem. 60 (1988) 1193–1202.
[38] W. Windig, J. Guilment, Interactive self-modeling mixture analysis, Anal. Chem. 63 (1991) 1425–1432.
[39] E. Spjotvoll, H. Martens, R. Volden, Restricted least squares estimation of the spectra and concentration of two unknown constituents available in mixtures, Technometrics 24 (1982) 173–180.
[40] J. Jaumot, R. Tauler, MCR-BANDS: a user friendly MATLAB program for the evaluation of rotation ambiguities in multivariate curve resolution, Chemom. Intell. Lab. Syst. 103 (2010) 96–107.
[41] R. Bro, PARAFAC, Tutorial and applications, Chemom. Intell. Lab. Syst. 38 (1997) 149–171.
[42] A. Savitzky, M.J.E. Golay., Smoothing and differentiation of data by simplified least sqares procedures, Anal. Chem. 36 (1964) 1627–1639.
[43] The MathWorks Inc., MATLAB 7.6, The MathWorks Inc., Natick, Massachussets, USA 2008, p. 6.
[44] A.C. Olivieri, H.L. Wu, R.Q. Yu., MVC3: a MATLAB graphical interface toolbox for third-order multivariate calibration, Chemom. Intell. Lab. Syst. 116 (2012) 9–16.
[45] R. Bro, H.A.L. Kiers., A new efficient method for determining the number of components in PARAFAC models, J. Chemom. 17 (2003) 274–286.
[46] M.J. Culzoni, H.C. Goicoechea, M. Bearzoti, M. Cabezón, A.C. Olivieri, Evaluation of partial least-squares with second-order advantage for the multi-way spectroscopic analysis of complex biological samples in the presence of analyte-background interactions, Analyst 131 (2006) 718–723.
[47] J. Riu, F.X. Rius, Method comparison using regression with uncertainties in both axes, Trends Anal. Chem. 16 (1997) 211–216.
[48] C. Bauza, G.A. Ibañez, R. Tauler, A.C. Olivieri, Sensitivity equation for quantitative analysis with multivariate curve resolution-alternating least-squares: theoretical and experimental approach, Anal. Chem. 84 (2012) 8697–8706.
[49] F.A. Allegrini, A.C. Olivieri, Analytical figures of merit for partial least-squares coupled to residual multilinearization, Anal. Chem. 84 (2012) 10823–10830.